# MULTIFUNCTIONAL FILMS FOR FUSION BONDING AND STRUCTURAL HEALTH MONITORING OF THERMOPLASTIC COMPOSITE JOINTS

H. Frederick[a], W. Li[a], W. Sands[b], E. Tsai[c] and G. Palardy[a*]

[a] Department of Mechanical and Industrial Engineering, Louisiana State University
3261 Patrick F. Taylor Hall
Baton Rouge, LA 70803

[b] Materials Science and Engineering, Clemson University
161 Sirrine Hall
Clemson, SC 29634

[c] Department of Chemistry, Louisiana State University
232 Choppin Hall
Baton Rouge, LA 70803

## ABSTRACT

Ultrasonic welding is a promising method to quickly bond thermoplastic composite parts. In this process, a thermoplastic film, called an "energy director", is placed between two pieces of composite materials, and melted during the welding process to facilitate bonding. This study seeks to develop a multifunctional energy director suitable for three purposes: 1) ultrasonic welding, 2) structural health monitoring (SHM) via electrical resistance measurements, and 3) heating element for disassembly and repair of the damaged bond. Various materials and manufacturing methods were investigated to develop multifunctional films: 1) magnetic or conductive nanoparticles deposited onto polymer films, and 2) multi-walled carbon nanotubes (MWNTs) dispersed into polymers. The latter was selected as a promising candidate because of its ease of manufacturability through compression molding and its compatibility with the welding process. The thermo-electrical and electro-mechanical behavior of compression molded films containing up to 20 wt% MWNT in a polypropylene (PP) matrix was assessed via a sourcemeter and dynamic mechanical analyzer. To demonstrate multifunctionality, glass fiber/PP specimens were ultrasonically welded with the MWNT/PP films as energy directors. While the multifunctional films reduced lap shear strength by up to 10%, they did not significantly affect the welding process. Moreover, welded specimens with the MWNT/PP films were successfully tested under cyclic bending for SHM through resistance measurements.

Corresponding author: Genevieve Palardy (gpalardy@lsu.edu)

*Copyright 2020. Used by the Society of the Advancement of Material and Process Engineering with permission.*

*SAMPE Virtual Conference Proceedings, 2020. Society for the Advancement of Material and Process Engineering – North America.*

# 1. INTRODUCTION

Lightweight composite materials are of great interest in several fields of applications, especially aerospace and ground transportation. The most popular types of conventional fiber-reinforced composites are thermoset composites (TSCs) and thermoplastic composites (TPCs). The main difference between thermoset and thermoplastic polymers is that the latter soften and may be formed again when heated up above a certain temperature. This makes thermoplastic composites more sustainable in the long-term as they can be reused and recycled. An additional benefit is that they can be joined through fusion bonding, otherwise known as "welding", eliminating the use of mechanical fasteners [1]. This feature makes them competitive for high-end, high-performance sectors where the weight reduction translates into important cost savings.

An upcoming joining technique for fiber-reinforced thermoplastic composites, ultrasonic welding (USW), is generating considerable interest, most particularly in the aerospace and automotive industries due to its fast cycle times and flexibility [2]. While this technique has been successfully demonstrated on lab-scale and medium-sized composite structures, most research is directed toward process development and optimization through static strength data [3-7]. There is still a lack of confidence, notably, in the fundamental prediction of failure behavior at the joint. In order for ultrasonically welded composite joints to be considered in industrial applications, it is imperative to find innovative ways to enable structural health monitoring (SHM), as well as predict loading and failure modes.

SHM of thermoset composites and adhesive joints is a popular field of research, but welded TPC joints are not widely studied [8, 9]. This work aims to integrate multifunctional films at the interface of ultrasonically welded thermoplastic composites, which would serve three purposes, as illustrated in Figure 1: i) energy director to enable ultrasonic welding, ii) sensor to monitor strains, and iii) heating element for disassembly and repair. Promising multifunctional films for strain sensing and self-heating are nanocomposite-based, where electrically conductive nanoparticles/nanofibers (e.g. carbon nanotubes (CNTs), CNT buckypaper) are combined with a polymer matrix [10-13]. However, an additional challenge unique to the USW process, over other common fusion bonding methods, is the application of vibrations disrupting the interface to be joined. As the interface melts, polymer is squeezed out in less than 1 second, meaning fragile sensors (e.g. optical fibers) or geometrically sensitive sensors (e.g. 3D printed patterns) are not suitable.

This paper focuses on multifunctional films characterization, ultrasonic welding and structural health monitoring of welded joints under bending (Figure 1). It will first summarize the preparation methods that have been investigated to create multifunctional films suitable for USW. Second, it will present thermo-electrical and electro-mechanical characterization of the most suitable films, through resistance heating and dynamic mechanical analysis (DMA). Third, the effect of multifunctional films on welded TPC samples will be assessed through welding curves, outputs and lap shear strength. Finally, potential for SHM will be demonstrated during periodic bending of welded joints in a single lap configuration.

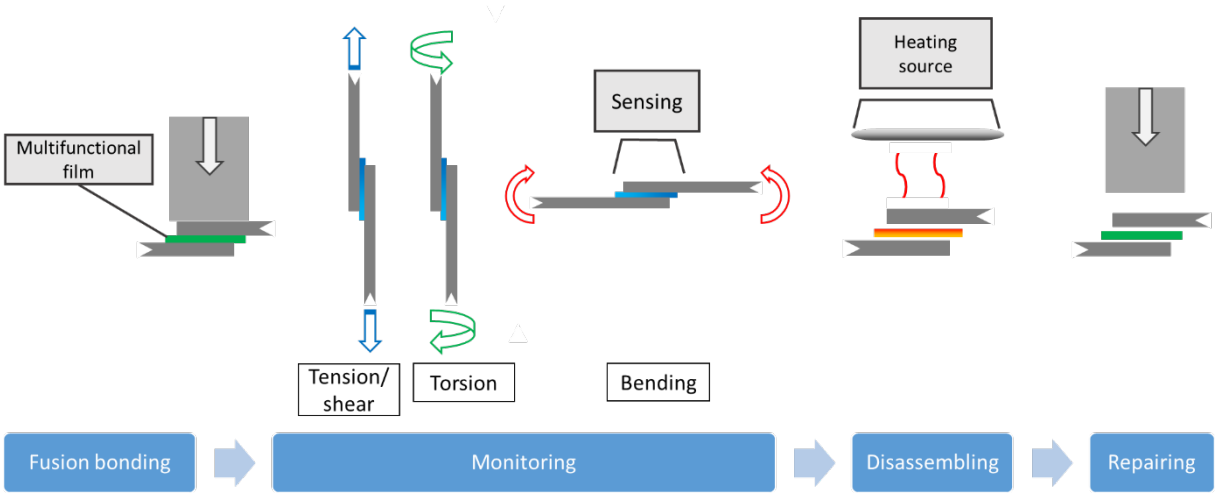



Figure 1. Global, long-term vision for the proposed research. The current paper focuses on multifunctional films characterization, fusion bonding and structural health monitoring of welded joints under bending.

# 2. EXPERIMENTATION

## 2.1 Materials and manufacturing for multifunctional films

Several materials and manufacturing methods were considered in this study, as listed in Table 1. Five types of polymers were investigated: PP, PA6, PEI, PPS and PEEK (see below Table 1 for definitions). Electrically conductive and magnetic nanoparticles were used: silver and iron oxide nanoparticles in aqueous or hexane solutions, and multi-walled carbon nanotubes (MWNT) dispersed in polymer pellets (masterbatches). Those particles were considered because strain monitoring can be carried out through resistance measurements and self-heating through resistance or induction heating.

Two manufacturing methods were explored: 1) drop casting, and 2) compression molding. Drop casting is depicted in Figure 2 and was studied first for its ease of implementation, versatility, low cost and demonstrated use for induction welding of TPCs [14]. It consists of depositing drops of a solution containing dispersed nanoparticles on a polymer film, then placing the film in an oven or on a hot plate to evaporate the solvent (at temperatures listed in Table 1). Nanoparticles were diluted to concentrations between 2,000 ppm and 30,000 ppm. One to three layers were deposited on the polymer films. The quality of the films was visually assessed and observed under scanning electron microscope (SEM) for defects.

The second film manufacturing method, compression molding, consists of placing thermoplastic pellets, granules or powder containing nanoparticles (masterbatches) on a heated hydraulic press and increasing the pressure to form films. To test out film manufacturing and potential for multifunctionality, commercial masterbatches were purchased as listed in Table 1. MWNT were selected because of their electrical properties and availability as masterbatches with a wide range of thermoplastics. PP masterbatches containing 15 wt% and 20 wt% MWNT were chosen based on their low melting temperature and cost to demonstrate strain sensing/self-heating capabilities with welded PP composites. Stainless steel shims were used to manufacture films with three thickness values: 0.06 mm, 0.25 mm and 0.50 mm. Those values were selected based on previous

research on ultrasonic welding of thermoplastic composites [15]. The films were then cut into rectangular strips for characterization and ultrasonic welding.

Table 1. Materials and manufacturing methods considered for multifunctional films.

| Polymers | Nanoparticles | Manufacturing methods |
|---|---|---|
| PA6[1], PEI[2], PPS[3], PEEK[4] (0.07 mm to 0.25 mm-thick films) | Silver nanoparticles in aqueous solution[6] | Dilution to concentrations from 2,000 to 30,000 ppm Drop casting + oven heating between 50 °C and 90 °C |
| | Magnetic nanoparticles (iron oxide) in aqueous solution[7] | |
| | Magnetic nanoparticles (iron oxide) in hexane[8] | |
| PP[5] (pellets) | MWNT[9] (15 wt% and 20 wt%) | Compression molding at 170-200 °C for 15 min |

[1]Polyamide 6 (Goodfellow), [2]Poly ether imide (ULTEM®, McMaster-Carr), [3]Poly phenylene sulphide (Fortron®, CS Hyde Company), [4]Poly ether ether ketone (McMaster-Carr), [5]Polypropylene (pure pellets purchased from Goodfellow), [6]Purchased from US Research Nanomaterials, Inc., [7]Iron(II,III) oxide nanopowder with 50-100 nm particle size (Sigma-Aldrich), [8]Nanoparticles synthesized and provided by Dr. James Dorman and Natalia Da Silva Moura (Department of Chemical Engineering, LSU), [9]Multi-walled carbon nanotubes masterbatches (Cheap Tubes Inc.).

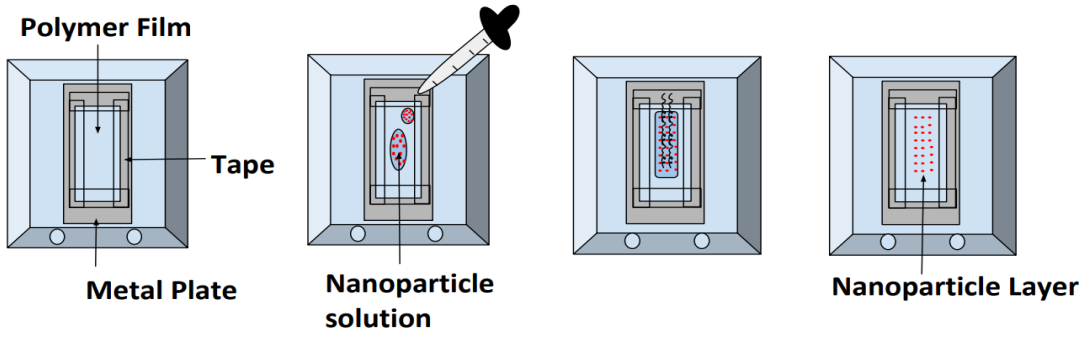



Figure 2. Film preparation using the drop casting method.

## 2.2 Materials and manufacturing for thermoplastic composites

In this study, glass fiber/polypropylene (GF/PP) 6030 unitape Polystrand™ (PolyOne) prepregs were used. A laminate with 1.86 mm final thickness, manufactured by placing eight GF/PP prepreg layers (0.33 mm thickness for each layer) in 0° orientation, was consolidated by hot pressing at 180 °C and 1 MPa for 15 min. After cooling, 101.6 mm × 25.4 mm rectangular strips were cut with a PICO 155 Precision Saw (Pace Technologies), with the longest dimension along the direction of the fibers.

## 2.3 Thermo-electrical and electro-mechanical characterization of multifunctional films

For electrical resistance and resistance heating tests, a voltage was applied through copper electrodes placed at both ends of the films with a Keithley Sourcemeter 2604B. It has a maximum

voltage and current of 40 V and 1 A, respectively. Temperature during resistance heating was measured with a FLIR A325sc camera placed above the film. The DC voltages used to gather electrical and thermo-electrical data were 1 V, 2 V, 4 V, 6 V, 8 V, and 10 V. Each test was carried out on five film samples over a period of three minutes while the Keithley KickStart software acquired resistance, power and current data.

To determine if the films can be used as strain sensors, electro-mechanical characterization was carried out in a dynamic mechanical analyzer (DMA Q800, TA Instruments). The films were clamped with the tension fixture while electrodes from the Keithley Sourcemeter were attached to the steel grips of the DMA. For these tests, a constant 4 V was applied to the films. The loading cycles applied 1 N to 15 N tensile force, in 1 N increments, at a rate of 3 N/min. For each cycle, once the load was fully applied or removed, it was held constant for 30 seconds. Strain and stress curves were monitored at the same time as resistance change.

### 2.4 Ultrasonic welding of thermoplastic composite joints

A Dynamic 3000 ultrasonic welder (RINCO ULTRASONICS AG) with a 40 mm diameter sonotrode was used to weld samples in a single lap configuration with an overlap of 25.4 mm × 12.7 mm. This microprocessor-controlled ultrasonic welder has a maximum power of 3000 W and is operated at a frequency of 20 kHz. Two custom-designed clamps were used to prevent bending of the top adherend, while allowing its vertical displacement. As Figure 3 shows, samples consisting of a top adherend, bottom adherend and 0.5 mm-thick multifunctional film (also referred to as flat energy director (ED)) were welded. PP EDs were used (pure PP, 15 wt%, and 20 wt% MWNT), as listed in Table 1. The vibration amplitude was set to 38.1 μm and a welding force of 1000 N was used for all welds. Solidification force and holding time were set to 1000 N and 4000 ms, respectively. Three different vertical displacement values (also known as “travel”) were chosen: 40%, 60%, and 80% of the initial film thickness. After welding, the ultrasonic welder output four main parameters: vibration time (ms), energy (J), maximum power (%), and weld distance (mm). In addition, power and travel curves were extracted from the welding data. For each travel and ED type, five samples were welded.

### 2.5 Mechanical testing of welded joints

After welding, tensile testing was carried out by using a 25 kN test machine (TestResources 313) for lap shear strength (LSS), according to the ASTM D1002 standard. Single-lap joint samples were clamped by hydraulic wedge grips at a distance of 60 mm and a loading rate of 1.3 mm/min. LSS was obtained by dividing the maximum load ($F_{max}$) by the overlap area (25.4 mm × 12.7 mm). Fracture surfaces and failure modes were observed through visual inspection. Three to five samples were tested for each ED type and travel value.

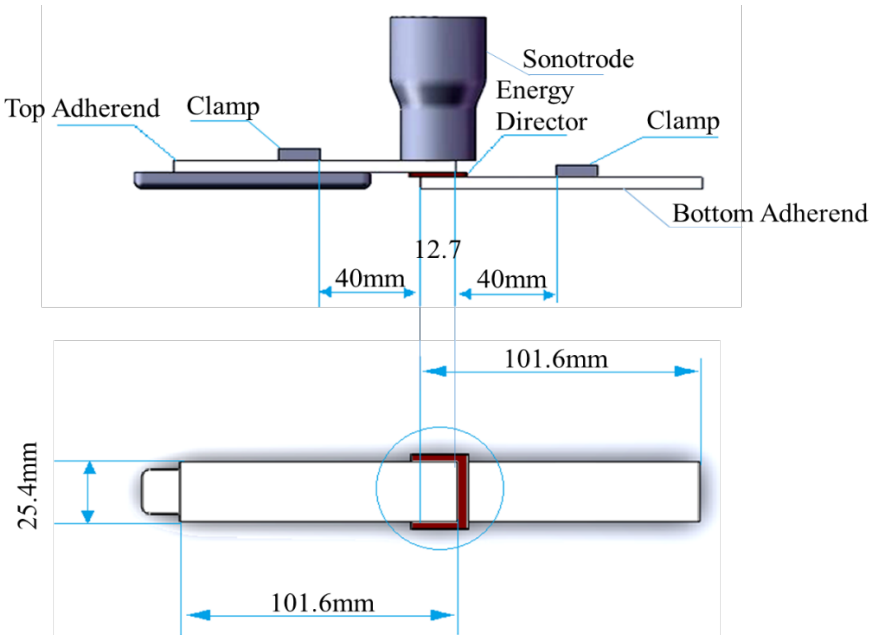



Figure 3. Schematic of the welded samples used in this study (all dimensions are in mm).

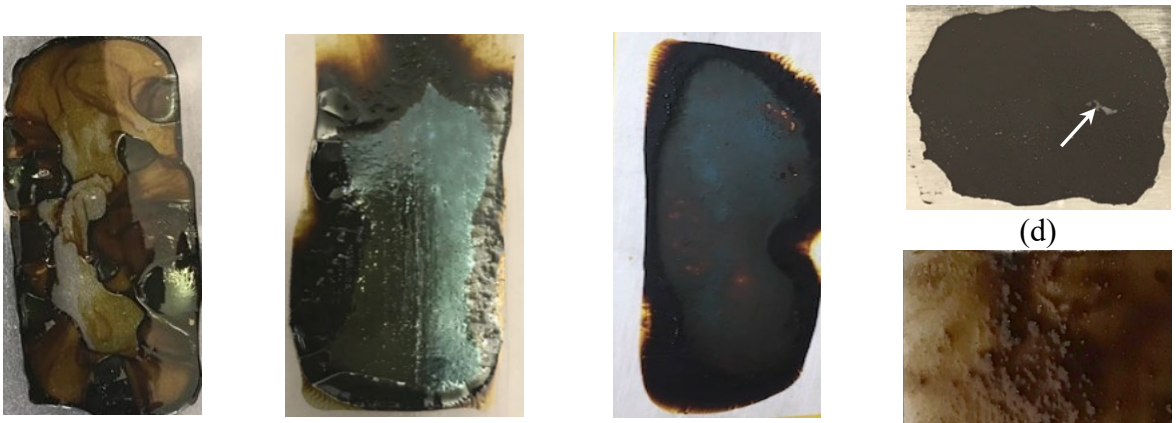
### 2.6 Structural health monitoring of welded joints

Samples welded with 15 wt% and 20 wt% MWNT/PP films at 60% and 80% travel were monitored in bending tests. Before testing, silver conductive paint (SPI #05002-AB) was applied on both sides of the overlap parallel to the direction of the fibers. Two 30 AWG copper wires were placed on the silver coating before drying and fixed with adhesive flash tape. Samples were dried overnight at room temperature. A vise grip was used to hold the welded samples in place and a downward load was periodically applied at 35 s intervals at the end of the cantilever beam with a maximum vertical displacement of 50 mm. Samples were held for 3 s at the maximum displacement before releasing the load. A Keithley Sourcemeter 2604B was used to apply a voltage of 3 V and measure resistance during bending. Resistance curves were recorded using the Keithley KickStart software.

## 3. RESULTS

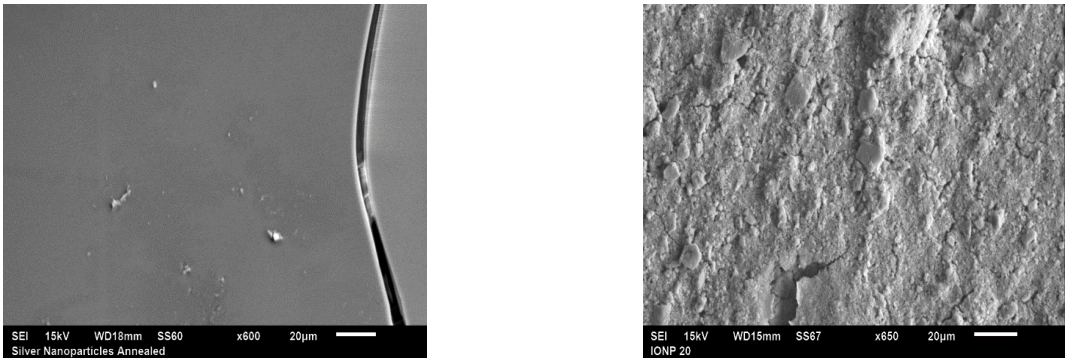
### 3.1 Multifunctional film fabrication and selection

Figure 4 shows representative examples of the films created by drop casting. Polymers with the lowest glass transition temperature, such as PA6, were not well suited for this method: the films warped during the evaporation process as the temperature was close or above their glass transition. This resulted in uneven nanoparticle distribution and thickness, as seen in Figure 4a. More consistent films were produced with PEEK (Figure 4b), PEI (Figure 4c) and PPS. Magnetic particles dispersed in an aqueous solution also produced generally uniform layers on the polymer films (Figure 4d), but appeared brittle with low adhesion to the substrate, as indicated by the white arrow. Iron oxide nanoparticles in hexane (Figure 4e), while allowing for the highest dispersed concentration, left an oily residue after evaporation. SEM images showed micro-cracks in the films containing silver nanoparticles (Figure 5a) and confirmed brittleness of the iron oxide nanoparticles films with poor adhesion to the substrate (Figure 5b).



(a) (b) (c) (d) (e)

Figure 4. Examples of films coated with nanoparticles with the drop casting method: a) silver nanoparticles on PA6 film, b) silver nanoparticles on PEEK film, c) silver nanoparticles on PEI, d) magnetic nanoparticles on PEI film, and e) synthesized iron oxide nanoparticles dispersed in hexane on PEI. The white arrow on d) indicated a missing piece of film due to brittleness and poor adhesion to the substrate.




(a) (b)

Figure 5. SEM images of drop cast films with: a) silver nanoparticles (Figure 3b), and b) synthesized iron oxide nanoparticles (Figure 3e). Scale bar: 20 µm.

While the drop casting method was a versatile and low cost technique, it possessed several disadvantages:

1) If the glass transition temperature of the polymer films was below 100 $^{o}$C, film distortion occurred during the evaporation phase;
2) In many cases, nanoparticle layers were uneven in both distribution and thickness (see Figure 4a - c);
3) Nanoparticle layers were brittle with low adhesion with the polymer films:
   a) Silver nanoparticles produced a solid layer, but the latter cracked easily, separating itself from the substrate;
   b) Magnetic nanoparticles dispersed in an aqueous solution produced even layers, but poor adhesion made it difficult to maintain their integrity;
4) Magnetic nanoparticles dispersed in hexane produced even layers, but hexane, when evaporated, left an oily residue, which would not be suitable to bond interfaces.

In addition, due to the brittleness and low adhesion of the nanoparticle layers, this manufacturing method would not be suitable for the ultrasonic welding process. The layers' integrity might be compromised under ultrasonic vibrations, rendering the strain sensing and disassembly capabilities ineffective.

On the other hand, compression molding produced films with consistent thickness with nanoparticles directly embedded and dispersed into the polymer matrix. One potential downside was the films' brittleness, depending on the polymer (crystallinity) and thermal history. When re-pressed more than once, the polymer films became more brittle. Nonetheless, this manufacturing method was considered suitable to proceed further in this project.

## 3.2 Multifunctional PP/MWNT films characterization

### *3.2.1 Thermo-electrical behavior*

Figure 6 shows representative results for conductivity measurements of PP films containing 15 wt% and 20 wt% MWNT. As the voltage increased, average conductivity and standard deviation both decreased. Generally, electrical conductivity converged below 6 S/m for both films, with a higher value for 20 wt% MWNT, as expected from the denser conductive path network. It is in the same order of magnitude as previously observed in the literature for MWNT polymer films [12].

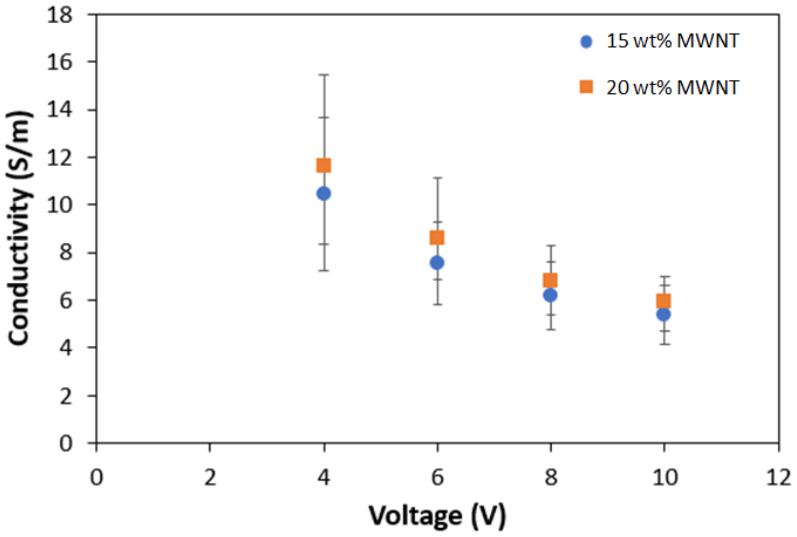



Figure 6. Representative average electrical conductivity of 15 wt% MWNT/PP and 20 wt% MWNT/PP films at different voltage values.

Figure 7 was obtained by plotting the average maximum temperature of the three film thicknesses containing 20 wt% MWNT. This data shows that little to no heating occurred with an input voltage of 4 V while, in some experiments, an input of 10 V caused the film temperature to reach values above 120 ºC, approaching the melting temperature of polypropylene (160 ºC). While there is some deviation from sample to sample, most likely due to the temperatures not being normalized for geometric differences, it can be seen that the thicker films tended to reach a higher temperature. A similar behavior was observed for 15 wt% MWNT films, with a maximum average temperature

of 114ºC. Further tests will be carried out at higher voltages to assess potential for disassembly and repair when the films are used as energy directors in ultrasonic welding. For electro-mechanical tests, a maximum voltage equal to 4 was selected to eliminate potential resistance change caused by the temperature [12].

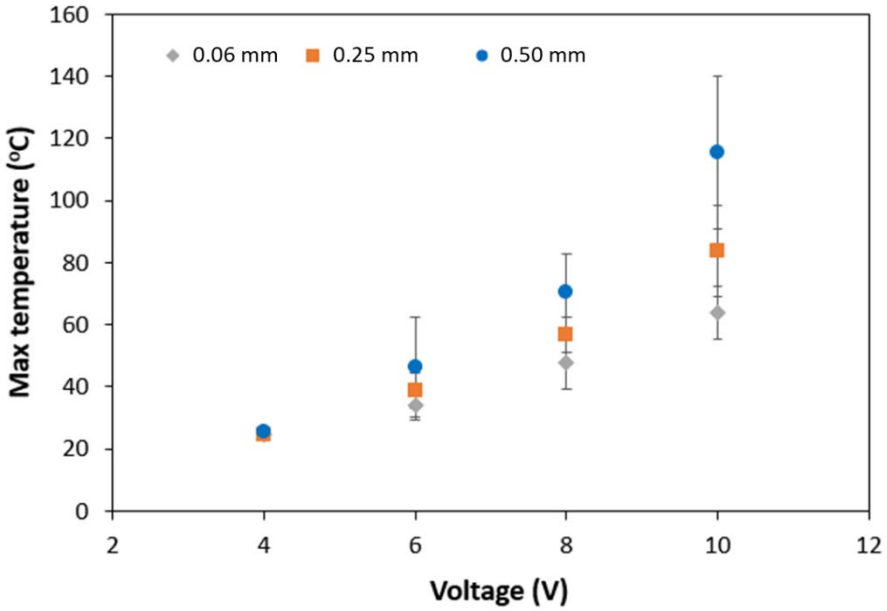



Figure 7. Average maximum temperature of 20 wt% MWNT/PP films with three thicknesses: 0.06 mm, 0.25 mm and 0.50 mm.

### *3.2.2 Electro-mechanical behavior with DMA*

Films containing 15 wt% and 20 wt% MWNT were tested under tension in a DMA. Figure 8 shows representative results for one complete test run. As the films were strained, the resistance followed a similar cyclic behavior for both specimens. This behavior was however not noticeable below 0.1% strain. Comparing the two MWNT content values, the signal for the 20 wt% film appeared more sensitive to low strains while also maintaining a more consistent resistance reading.

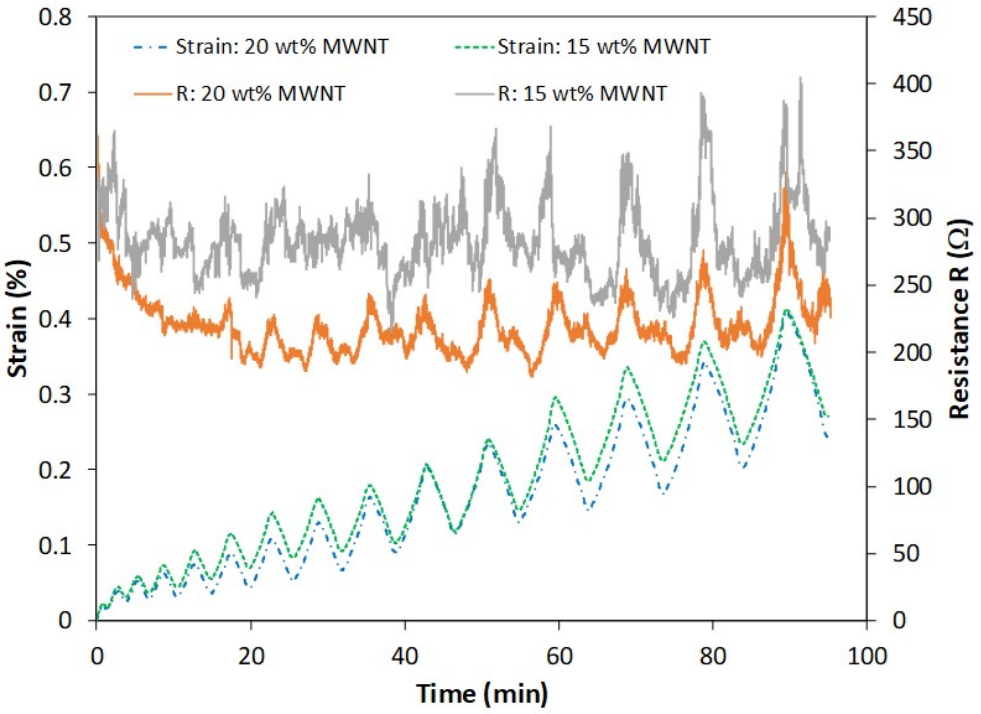



Figure 8. Relationship between strain and resistance of 15 wt% and 20 wt% MWNT/PP films.

## 3.3 Ultrasonically welded thermoplastic composite joints

### *3.3.1 Effect of multifunctional films on welding process*

Typical power and displacement curves for welded samples at 60% travel with all three types of EDs (pure PP, 15 wt% and 20 wt% MWNT) are shown in Figure 9. A positive displacement value represents downward movement of the sonotrode. The shape of the displacement curves follows a similar behavior as seen in the literature, as the energy director is squeezed out at the interface [3, 15]. Table 2 compares the average values of vibration time (US-time), energy, and maximum power (out of 3000 W) for samples welded under different conditions. Generally, as the travel increased, time, energy and power increased as well. An increase in MWNT content resulted into nominal changes in the output values, suggesting that the multifunctional energy directors did not significantly affect the welding process.

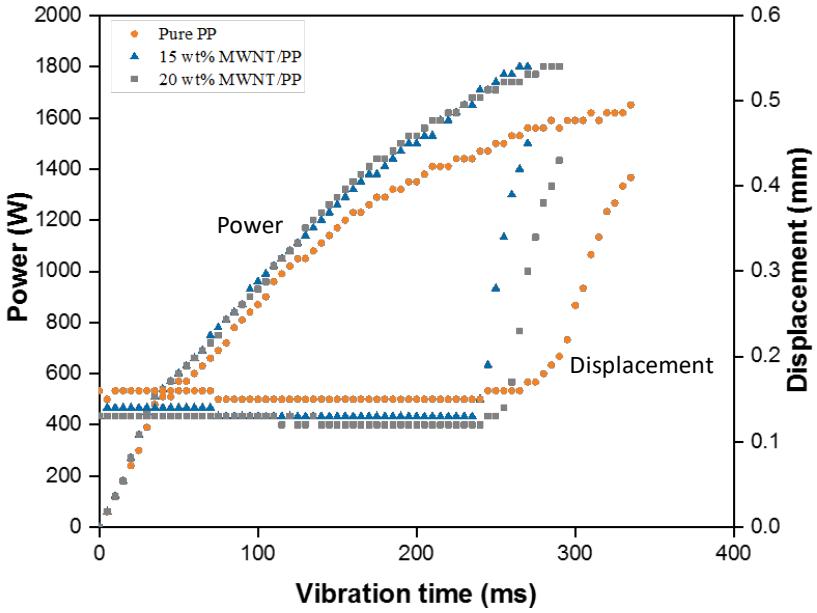



Figure 9. Comparison of power and displacement curves for GF/PP samples welded with pure PP films (circular), 15% wt MWNT/PP films (triangle), and 20 wt% MWNT/PP films (square) at 60% travel.

Table 2. Average values for vibration time (US-time), energy, and maximum power.

| Welding Output / Welding Travel | US-Time (ms) | Energy (J) | Maximum Power (%) |
|---|---|---|---|
| **40% (pure PP)** | 330 (±28) | 316 (±22) | 56 (±2) |
| **60% (pure PP)** | 357 (±15) | 366 (±11) | 59 (±3) |
| **60% (15 wt% MWNT)** | 311 (±11) | 309 (±12) | 58 (±2) |
| **60% (20 wt% MWNT)** | 321 (±22) | 321 (±44) | 59 (±2) |
| **80% (pure PP)** | 383 (±22) | 406 (±38) | 60 (±3) |
| **80% (15 wt% MWNT)** | 384 (±10) | 425 (±28) | 59 (±2) |
| **80% (20 wt% MWNT)** | 404 (±35) | 473 (±46) | 63 (±3) |

### *3.3.2 Effect of multifunctional films on lap shear strength and failure modes*

Average lap shear strength (LSS) values versus travel for the three different EDs are shown in Figure 10. A maximum LSS of 14.9 ± 1.59 MPa was obtained for GF/PP samples with pure PP films at 80% travel. Overall, pure PP EDs led to slightly higher LSS compared to multifunctional films. The lowest LSS values were obtained with 15 wt% MWNT films. Their average LSS was 9.8% lower at 60% travel and 9.4% lower at 80% travel, respectively, compared with pure PP films. A comparison of fracture surfaces between pure PP, 15 wt% MWNT, and 20 wt% MWNT films at 80% travel is shown in Figure 11. Generally, failure within the top ply of the substrates was observed for all samples, but fibers were deformed and squeezed out to the sides for both 15 wt% and 20 wt% MWNT films. This may have led to a decrease in LSS, compared to pure PP

films, as observed in Figure 10. Nonetheless, multifunctional films did not significantly influence the weld quality or output parameters, with a maximum LSS decrease below 10%.

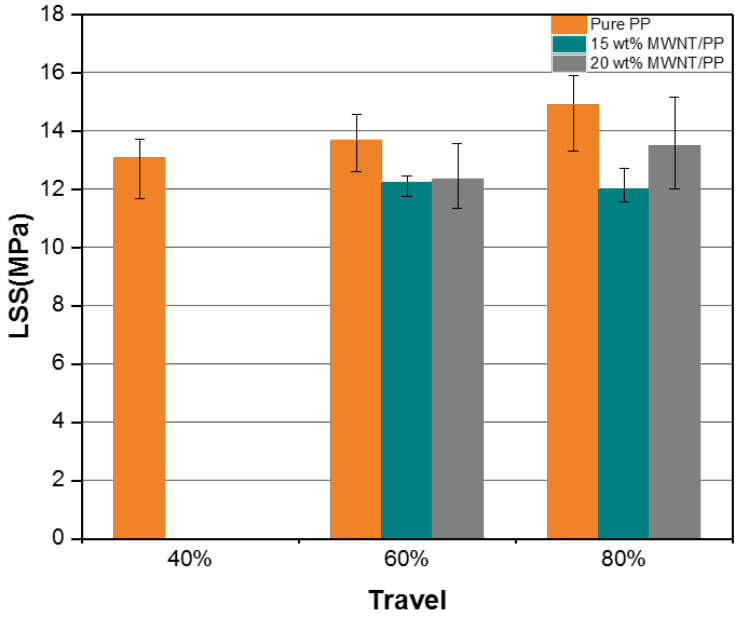



Figure 10. Comparison between the LSS of pure PP (orange), 15 wt% MWNT/PP (blue), and 20 wt% MWNT/PP (gray) films at 40%, 60%, and 80% travel.

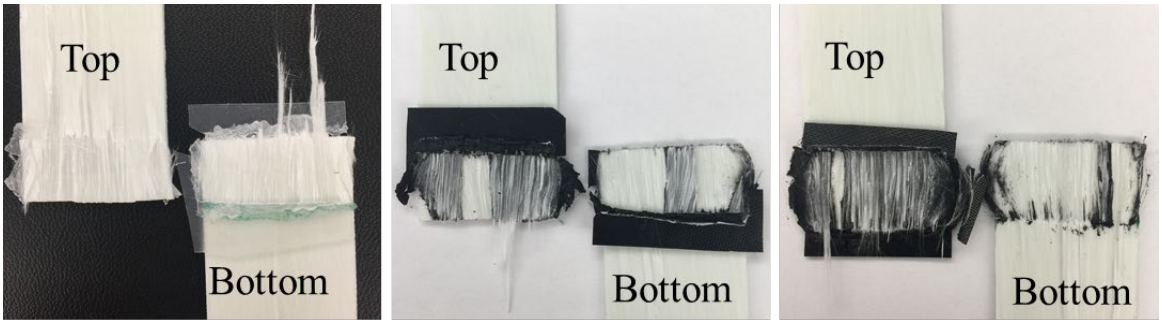



Figure 11. Representative fracture surfaces for GF/PP samples welded at 80% travel: pure PP films (left), 15 wt% MWNT films (middle), and 20 wt% MWNT films (right).

### *3.3.3 Potential for structural health monitoring*

GF/PP samples welded according to 60% and 80% travel were tested in bending for structural health monitoring. Figure 12 shows representative curves for the measured resistance for welded joints at 60% travel, under the influence of periodic pressure, as explained in Section 2.5. It is observed, for both 15 wt% and 20 wt% MWNT films, that resistance changed with the application of external displacement, in the order of 0.2 Ω. This behavior was also observed in the literature for buckypaper-based sensors embedded into carbon fiber/epoxy rectangular samples subjected to bending [10]. Similarly to the samples tested in the DMA (Figure 8), multifunctional films with a higher MWNT content displayed more consistent readings. Overall, the films proposed in this

study show promise as strain sensors for structural health monitoring of ultrasonically welded thermoplastic composite joints.

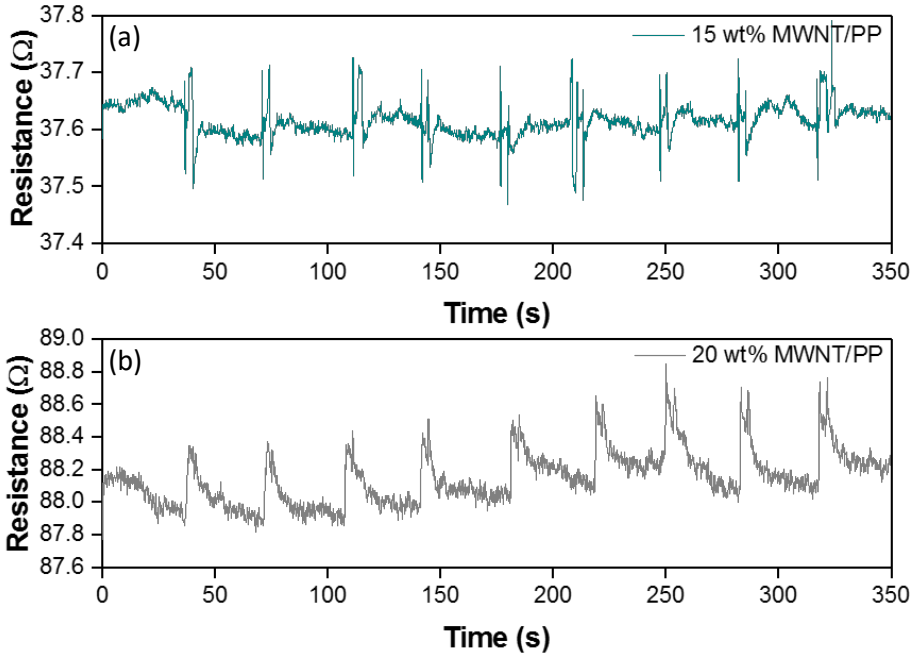



Figure 12. Representative curves for resistance versus time with periodic bending: (a) 20 wt% MWNT/PP films at 60% travel; (b) 15 wt% MWNT/PP films at 60% travel.

## 4. CONCLUSIONS

In this paper, the potential of various multifunctional polymer films for structural health monitoring of ultrasonically welded thermoplastic composite joints was investigated. The following observations and conclusions were noted:

- Compression molding is a simple method leading to high quality films with even thickness. Drop casting, on the other hand, produced films with uneven nanoparticles distribution, with poor adhesion to the polymer substrates, not suitable for ultrasonic welding.
- Thermo-electrical characterization of MWNT/PP films showed that a maximum temperature above 120 ºC was reached with 20 wt% MWNT at 10 V. It would be possible to reach higher temperatures for disassembly and repair of welded joints at higher voltage.
- Electro-mechanical behavior of the films was assessed under cyclic tensile loading in a DMA. Films containing 20 wt% MWNT were more sensitive to low strains and displayed a more consistent resistance reading.
- Multifunctional films did not significantly influence the welding outputs (time, energy and power). Lap shear strength varied between 12.0 MPa and 14.9 MPa. It decreased by a maximum of 10% for EDs containing 15 wt% MWNT, compared to samples welded with pure PP EDs. Fracture surface analysis revealed failure in the top ply of the adherends, but deformed fibers, squeezed out to the sides, for samples welded with 15 wt% and 20 wt% MWNT EDs may explain lower LSS values.

- The potential for SHM of welded joints using MWNT films was demonstrated through cyclic bending tests. A change of resistance at the welded interface was measured according to the cyclic application of an external displacement in bending.

Future directions include several topics: i) DMA cantilever beam testing of welded interfaces with resistance monitoring, ii) better understanding of failure modes for welded samples with multifunctional energy directors, iii) evaluation of the effect of bond thickness (travel parameter) on SHM capabilities, iv) structural health monitoring of welded GF/PP samples until failure for bending, tension and torsion tests, and v) assessment of ED's sensitivity as strain sensors and comparison with CNT buckypaper-based films.

## 5. REFERENCES


1. Yousefpour A, Hojjati M, Immarigeon J-P. "Fusion Bonding/Welding of Thermoplastic Composites". *Journal of Thermoplastic Composite Materials.* 2004;17(4):303-41.DOI:10.1177/0892705704045187
2. Palardy G, Shi H, Levy A, Le Corre S, Fernandez Villegas I. "A study on amplitude transmission in ultrasonic welding of thermoplastic composites". *Composites Part A: Applied Science and Manufacturing*. 2018;113:339-49.DOI:10.1016/j.compositesa.2018.07.033
3. Villegas IF. "In situ monitoring of ultrasonic welding of thermoplastic composites through power and displacement data". *Journal of Thermoplastic Composite Materials*. 2015;28(1):66-85. DOI:10.1177/0892705712475015
4. Goto K, Imai K, Arai M, Ishikawa T. "Shear and tensile joint strengths of carbon fiber-reinforced thermoplastics using ultrasonic welding". *Composites Part A: Applied Science and Manufacturing*. 2019;116:126-37.DOI:10.1016/j.compositesa.2018.10.032
5. Li Y, Arinez J, Liu Z, Hwa Lee T, Fan H-T, Xiao G, et al. "Ultrasonic Welding of Carbon Fiber Reinforced Composite With Variable Blank Holding Force". *Journal of Manufacturing Science and Engineering*. 2018;140(9).DOI:10.1115/1.4040427
6. Zhao T, Palardy G, Villegas IF, Rans C, Martinez M, Benedictus R. "Mechanical behaviour of thermoplastic composites spot-welded and mechanically fastened joints: A preliminary comparison". *Composites Part B-Engineering*. 2017;112:224-34.DOI:10.1016/j.compositesb.2016.12.028
7. Zhao T, Broek C, Palardy G, Villegas IF, Benedictus R. "Towards robust sequential ultrasonic spot welding of thermoplastic composites: Welding process control strategy for consistent weld quality". *Composites Part A: Applied Science and Manufacturing*. 2018;109:355-67.DOI:10.1016/j.compositesa.2018.03.024
8. Shimada S, Tanaka H, Hasebe K, Hayashi N, Ochi Y, Matsui T, et al. "Ultrasonic welding of polymer optical fibres onto composite materials". *Electronics Letters* [Internet]. 2016; 52(17):[1472-4 pp.].DOI:10.1049/el.2016.0905
9. Ochôa P, Villegas IF, Groves RM, Benedictus R. "Diagnostic of manufacturing defects in ultrasonically welded thermoplastic composite joints using ultrasonic guided waves". *NDT & E International*. 2019;107:102126.DOI:10.1016/j.ndteint.2019.102126
10. Siddique S, Park JG, Andrei P, Liang R. "M3D aerosol jet printed buckypaper multifunctional sensors for composite structural health monitoring". *Results in Physics*. 2019;13. DOI:10.1016/j.rinp.2019.02.030

11. DeGraff J, Liang R, Le MQ, Capsal J-F, Ganet F, Cottinet P-J. "Printable low-cost and flexible carbon nanotube buckypaper motion sensors". *Materials & Design*. 2017;133:47-53.DOI:10.1016/j.matdes.2017.07.048
12. Jang S-H, Park Y-L. "Carbon nanotube-reinforced smart composites for sensing freezing temperature and deicing by self-heating". *Nanomaterials and Nanotechnology*. 2018;8.DOI:10.1177/1847980418776473
13. Costa P, Carvalho MF, Correia V, Viana JC, Lanceros-Mendez S. "Polymer Nanocomposite-Based Strain Sensors with Tailored Processability and Improved Device Integration". *ACS Applied Nano Materials*. 2018;1(6):3015-25.DOI:10.1021/acsanm.8b00647
14. Farahani RD, Janier M, Dubé M. "Conductive films of silver nanoparticles as novel susceptors for induction welding of thermoplastic composites". *Nanotechnology*. 2018;29(12):125701.DOI:10.1088/1361-6528/aaa93c
15. Palardy G, Villegas IF. "On the effect of flat energy directors thickness on heat generation during ultrasonic welding of thermoplastic composites". *Composite Interfaces*. 2016;24(2):203-14. DOI: 10.1080/09276440.2016.1199149